
LIA: Privacy-Preserving Data Quality Evaluation in Federated Learning Using a Lazy Influence Approximation

Ljubomir Rokvic¹, Panayiotis Danassis², Sai Praneeth Karimireddy³, Boi Faltings¹

¹École Polytechnique Fédérale de Lausanne (EPFL)

²Harvard University

³University of California, Berkeley

Abstract

In Federated Learning, it is crucial to handle low-quality, corrupted, or malicious data. However, traditional data valuation methods are not suitable due to privacy concerns. To address this, we propose a simple yet effective approach that utilizes a new influence approximation called "*lazy influence*" to filter and score data while preserving privacy. To do this, each participant uses their own data to estimate the influence of another participant's batch and sends a differentially private obfuscated score to the central coordinator. Our method has been shown to *successfully filter out biased and corrupted data* in various simulated and *real-world* settings, achieving a recall rate of over $> 90\%$ (sometimes up to 100%) while maintaining *strong differential privacy* guarantees with $\epsilon \leq 1$.

1 Introduction

The success of Machine Learning (ML) depends to a large extent on the availability of high-quality data [49]. Having the ability to *score* and *filter* irrelevant, noisy, or malicious data can significantly improve model accuracy and speed up training. However, ensuring data quality is especially challenging in Federated Learning (FL) [45, 32, 57]. In FL, a single *Center* uses data from independent and sometimes self-interested *data holders* to train a model jointly. Data holders often operate resource-constrained edge devices and include businesses and medical institutions that must protect the privacy of their data due to confidentiality or legal constraints. Thus, we never have direct access to the training data in order to inspect it, and privacy is a strong concern. This raises our main question: *how can we evaluate data quality in a distributed manner while preserving privacy?*

Imagine a collaborative project involving multiple hospitals across the globe, each with its own repository of chest X-ray scans of patients. The goal is to use FL to train a robust ML model capable of diagnosing heart conditions from these X-rays [51]. However, each hospital adheres to different data collection protocols. E.g., Hospital A may use a different scanner making it incompatible with the rest of the data. If included, it can lead to a large drop in accuracy [42]. More insidiously, Hospital B may habitually include textual annotations directly on the scans for internal communication. The model may rely on these shortcuts instead of looking at the actual scan [48].

To address these issues, we propose a "rite of passage" mechanism where a hospital's data is admitted into the FL system only if no issues are detected. By this, we not only ensure the integrity of the FL procedure, but can also flag potentially bad data-collection procedures for the hospitals. However, note that patient X-rays are very sensitive information and protected by strong privacy regulations such as HIPAA. Thus we need to ensure that both the model training and (for our purpose) more importantly the data quality assessment is performed in a federated and privacy preserving manner minimizing the patient information being leaked.

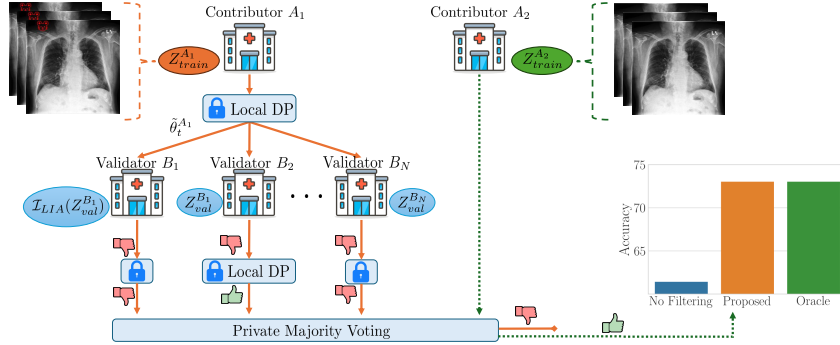


Figure 1: Data filtering procedure. Data contributors A_1 and A_2 want to join the federation, but might have biased or corrupted data (e.g., watermarks on A_1 X-rays). A_1 sends a differentially private (DP) partially updated model ($\tilde{\theta}_t^{A_1}$) to validators B_i , who submit a DP vote based on the performance they observe when using the model $\tilde{\theta}_t^{A_1}$ on their task (*Lazy Influence Approximation*). The aggregated votes are used as a ‘rite of passage’, to decide whether to incorporate A_1 ’s data. The same process happens for A_2 . A_2 is accepted in the federation, while A_1 is filtered out. Filtering can significantly improve the model’s accuracy from 61% (no filtering) to 73% (proposed), matching the performance of the optimal (oracle) filtering on diagnosing heart conditions from X-rays using *real-data* from [51].

A clean way of quantifying the quality of data point(s) is via the notion of *influence* [35, 11]. Intuitively, influence quantifies the marginal contribution of a data point (or batch of points) on a model’s accuracy. One can compute this by comparing the difference in the model’s empirical risk when trained with and without the point in question. While the influence metric can be highly informative, it is impractical to compute: re-training a model is time-consuming, costly, and often impossible, as participants do not have access to the entire dataset. We propose a simple and practical approximation of the *sign* of the exact influence (*Lazy Influence Approximation*) which is based on an estimate of the direction of the model after a small number of local training epochs with the new data.

The second challenge is to limit the information leaked by this approximate influence measure to preserve the privacy of the data. Many approaches to Federated Learning (e.g., [46, 55]) remedy this by combining FL with Differential Privacy (DP) [17–20, 31, 15, 9], a data anonymization technique that many researchers view as the gold standard [54]. We show how the sign of influence can be approximated in an FL setting while maintaining strong differential privacy guarantees. Specifically, there are two sets of participants’ data that we need to protect: the training and the validation data (see also Section 1.2). We use DP-SGD for this training to ensure datapoint-level local DP [1, 66] To ensure the privacy of the validation data and the influence approximation itself, we employ a differentially private defense mechanism based on the idea of randomized response [59] (inspired by [22]). Together the two mechanisms ensure strong, *worst-case differential privacy* guarantees while allowing for accurate data filtering. See Figure 1 for an overview of our approach.

1.1 Our Contributions

We address two major challenges in this work: (i) efficiently estimating the quality of a batch of training data, and (ii) keeping both the training and validation data used for this estimate private. For the former, we develop a novel metric called *Lazy Influence Approximation (LIA)*, while for the latter, we combine DP-SGD and a differentially-private voting scheme. More specifically:

- (1) We present a novel technique (**Lazy Influence Approximation**) for scoring and filtering data in Federated Learning.
- (2) We show that our proposed distributed influence aggregation scheme allows for **robust scoring, even under rigorous, worst-case differential privacy guarantees** (privacy cost $\epsilon < 1$). This is the recommended value in DP literature and much smaller than many other AI or ML applications.¹

¹AI or ML applications often assume ϵ as large as 10 [55] (see, e.g., [53]). For specific attacks, $\epsilon = 10$ means that an adversary can theoretically reach an accuracy of 99.99% [55]

(3) We evaluate our approach on four well-established datasets: CIFAR10, CIFAR100, *real-data* on Human Activity Recognition on edge devices [3], and *real-data* on diagnosing heart conditions from X-rays [51]. Our simulations include **two different modalities** (image and sensor data), and **corruption of both the input X , and the labels y** . We demonstrate that **filtering using our scheme can eliminate the adverse effects of inaccurate data**. We also show it can be easily combined with other robust-FL training methods, to further enhance the model’s performance.

1.2 High-Level Description of Our Setting

A center C coordinates a set of participants that contribute their data to train a single model (Figure 1). C has a small set of ‘warm-up’ data, which are used to train an initial model M_0 that captures the desired input/output relation. The model is then updated with the contributions of the participants. We assume that each data holder participant has a set of training points that will be used to improve the model and a set of validation points that will be used to evaluate other participants’ contributions. It must be kept private to prohibit participants from tailoring their contributions to the validation data. Each data holder participant can assume two roles: the role of the contributor (A) and the role of the validator (B). As a contributor, a participant performs a small number of local epochs to M_t – enough to get an estimate of the gradient² – using a batch of his training data $z_{A,t}$. Subsequently, A sends the updated partial model $M_{t,A}$, with specifically crafted noise to ensure DP, to the validators. The applied noise protects the updated gradient while still retaining information on the usefulness of data. Each validator B uses its validation dataset to approximate the empirical risk of A ’s training batch (i.e., the approximate influence). This is done by evaluating each validation point and comparing the loss. In an FL setting, we can not re-train the model to compute the exact influence; instead, B performs only a small number of training epochs, enough to estimate the direction of the model (Lazy Influence Approximation). As such, we look at the sign of the approximate influence (and not the magnitude). Each validator aggregates the signs of the influence for each validation point, applies controlled noise to ensure DP, and sends this information to the center. Finally, the center accepts A ’s training batch if most of the B s report positive influence and rejects otherwise (majority voting).

2 Related Work and Discussion

Federated Learning Federated Learning (FL) [45, 32, 57, 38] has emerged as an alternative method to train ML models on data obtained by many different agents. In FL, a center coordinates agents who acquire data and provide model updates. FL has been receiving increasing attention in both academia [39, 64, 26, 6] and industry [25, 8], with a plethora of real-world applications.

Influence functions Influence functions are a standard method from robust statistics [11] (see also Section 3), which were recently used as a method of explaining the predictions of black-box models [35]. They have also been used in the context of fast cross-validation in kernel methods and model robustness [43, 10]. While a powerful tool, computing the influence involves too much computation and communication, and it requires access to the training and validation data (see [35] and Section 3). There has also been recent work trying to combine Federated Learning with influence functions [62], though to the best of our knowledge, we are the first to provide a privacy-preserving alternative.

Data Filtering A common but computationally expensive approach for filtering in ML is to use the Shapley Value of the Influence to evaluate the quality of data [30, 23, 29, 63, 24, 60]. Other work includes, for example, rule-based filtering of least influential points [50], or constructing weighted data subsets (corsets) [14]. Because of the privacy requirements in FL, contributed data is not directly accessible for assessing its quality. [56] propose a decentralized filtering process specific to federated learning, yet they do not provide any formal privacy guarantees. While data filtering might not always pose a significant problem in traditional ML, in an FL setting, it is more important because even a small percentage of mislabeled data can result in a significant drop in the combined model’s accuracy.

Client Selection and Attack Detection Our setting can also be interpreted as potentially adversarial, but it should not be confused with Byzantine robustness. We do not consider threat scenarios as described in [7] and [52], where participants carefully craft malicious updates. Instead, we assume

²The number of local epochs is a hyperparameter. We do not need to train the model fully (e.g., 2-5 epochs).

that the data used for those updates might be corrupt. For completeness and in lack of more relevant baselines, we compare our work to two Byzantine robust methods: KRUM [5], Trimmed-mean [65], and Centered-Clipping [33] (along to an oracle filter). These methods, though, require gradients to be transmitted as is, i.e., they lack any formal privacy guarantee to the participants’ training data. Furthermore, both of these techniques require the center to know the number of malicious participants a priori. Nevertheless, we show that our approach can be combined with such robust-FL training methods, to further enhance the model’s performance.

Differential Privacy Differential Privacy (DP) [17–20] has emerged as the de facto standard for protecting the privacy of individuals. Informally, DP captures the increased risk to an individual’s privacy incurred by participating in the learning process. Consider a participant being surveyed on a sensitive topic as a simplified, intuitive example. To achieve differential privacy, one needs a source of randomness; thus, the participant decides to flip a coin. Depending on the result (heads or tails), the participant can reply truthfully or randomly. An attacker can not know if the decision was taken based on the participant’s preference or due to the coin toss. Of course, to get meaningful results, we need to bias the coin toward the actual data. In this simple example, the logarithm of the ratio $Pr[\text{heads}]/Pr[\text{tails}]$ represents the privacy cost (also referred to as the privacy budget), denoted traditionally by ϵ . Yet, one must be careful in designing a DP mechanism, as it is often hard to practically achieve a meaningful privacy guarantee (i.e., avoid adding a lot of noise and maintain high accuracy) [55, 13]. A variation of DP, instrumental in our context, given the decentralized nature of federated learning, is Local Differential Privacy (LDP) [34, 21]. LDP is a generalization of DP that assumes all communication between the data providers and the Center is public. Hence, we do not rely on the Center to take appropriate privacy measures and instead try limit information leakage in all communication. This allows us to work with untrusted central coordinators. An orthogonal concept is datapoint-level vs. user-level DP [58, 4, 44]. In user-level privacy, we attempt to protect datasets at the level of the data provider, rather than at the level of data-point. While this is typical in the cross-device FL where each data-provider represents the data of a single user, this does not make sense for multi-institutional collaboration [41]. In the setting we consider, each hospital (data provider) aggregates data from many patients. Thus, each user we want to protect is associated with a single data point, making datapoint-level DP more relevant. Thus, we consider datapoint-level local DP. We assume that the participants and the Center are *honest but curious*, i.e., they don’t actively attempt to corrupt the protocol but will try to learn about each other’s data.

3 Methodology

We aim to address two challenges: (i) approximating the influence of a (batch of) data point(s) without having to re-train the entire model from scratch and (ii) doing so while protecting the privacy of the training and validation data. The latter is essential not only to protect users’ sensitive information but also to ensure that malicious participants can not tailor their contributions to the validation data. We first introduce the notion of *influence* [11] and our proposed lazy approximation. Second, we describe a differentially private voting scheme for crowdsourcing the approximate influence values.

Setting We consider a classification problem from some input space \mathcal{X} (e.g., features, images, etc.) to an output space \mathcal{Y} (e.g., labels). In a FL setting, there is a center C that wants to learn a model $M(\theta)$ parameterized by $\theta \in \Theta$, with a non-negative loss function $L(z, \theta)$ on a sample $z = (\bar{x}, y) \in \mathcal{X} \times \mathcal{Y}$. Let $R(Z, \theta) = \frac{1}{n} \sum_{i=1}^n L(z_i, \theta)$ denote the empirical risk, given a set of data $Z = \{z_i\}_{i=1}^n$. We assume that the empirical risk is differentiable in θ .

Definitions In simple terms, influence measures the marginal contribution of a data point on a model’s accuracy. A positive influence value indicates that a data point improves model accuracy, and vice-versa. More specifically, let $Z = \{z_i\}_{i=1}^n$, $Z_{+j} = Z \cup z_j$ where $z_j \notin Z$, and let $\hat{R} = \min_{\theta} R(Z, \theta)$ and $\hat{R}_{+j} = \min_{\theta} R(Z_{+j}, \theta)$, where \hat{R} and \hat{R}_{+j} denote the minimum empirical risk of their respective set of data. The *influence* of datapoint z_j on Z is defined as $\mathcal{I}(z_j, Z) \triangleq \hat{R} - \hat{R}_{+j}$.

3.1 Shortcomings of the Exact and Approximate Influence in a FL Setting

Despite being highly informative, influence functions have not achieved widespread use in FL (or ML in general). This is mainly due to the computational cost. The exact influence requires complete

retraining of the model, which is time-consuming and very costly, especially for state-of-the-art, large ML models (importantly for our setting, we do not have direct access to the training data). Recently, the first-order Taylor approximation of influence [35] (based on [12]) has been proposed as a practical method to understanding the effects of training points on the predictions of a *centralized* ML model. While it can be computed without having to re-train the model, according to the following equation $\mathcal{I}_{appr}(z_j, z_{val}) \triangleq -\nabla_{\theta} L(z_{val}, \hat{\theta}) H_{\hat{\theta}}^{-1} \nabla_{\theta} L(z_j, \hat{\theta})$, it is still ill-matched for FL models for several key reasons.

Computing the influence approximation of [35] requires *forming and inverting* the Hessian of the empirical risk. With n training points and $\theta \in \mathbb{R}^m$, this requires $O(nm^2 + m^3)$ operations [35], which is *impractical* for modern-day deep neural networks with millions of parameters. To overcome these challenges, [35] used implicit Hessian-vector products (HVPs) to more efficiently approximate $\nabla_{\theta} L(z_{val}, \hat{\theta}) H_{\hat{\theta}}^{-1}$, which is typically $O(m)$. While this is a somewhat more efficient computation, it is *communication-intensive*, as it requires *transferring all of the (either training or validation) data* at each FL round. Most importantly, it *can not provide any privacy* to the users' data, an important, inherent requirement/constraint in FL. Finally, the loss function has to be strictly convex and twice differentiable (which is not always the case in modern ML applications). [35] proposed to swap out non-differentiable components for smoothed approximations, but there is no quality guarantee of the influence calculated in this way.

3.2 Lazy Influence (LIA): A Practical Influence Metric for Filtering Data in FL Applications

The key idea is that *we do not need to approximate the influence value* to filter data; we only need an accurate estimate of its *sign* (in expectation). Recall that a positive influence value indicates a data point improves model accuracy. Thus, we only need to approximate the sign of the loss and use that information to filter out data whose influence falls below a certain threshold.

Recall that each data holder participant may assume two roles: the role of the contributor (A) and the role of the validator (B). The proposed approach works as a 'rite of passage' for contributor A , arriving at round t . Our approach works as follows (Algorithm 1):

(i) At federated learning round t (model $M_t(\theta_t)$), the contributor participant A performs a small number k of local epochs to M_t using a batch of his training data $Z_{A,t}$, resulting in $\tilde{\theta}_t^A$. k is a hyperparameter. $\tilde{\theta}_t^A$ is the partially trained model of participant A , where most of the layers, except the last one, have been frozen. The model should not be fully trained for two key reasons: efficiency and avoiding over-fitting (e.g., in our simulations, we only performed 1-20 epochs). Furthermore, A adds noise to $\tilde{\theta}_t^A$ (see Section 3.2.2) to ensure strong, worst-case local differential privacy. Finally, A sends only the last layer (to reduce communication cost) of $\tilde{\theta}_t^A$ to every other participant.

(ii) Each validator B uses his validation dataset Z_{val}^B to estimate the sign of the influence using Equation 1. Next, the validator applies noise to $\mathcal{I}_{LIA}(Z_{val}^B)$, as described in Section 3.2.3, to ensure strong, worst-case differential privacy guarantees (i.e., keep his validation dataset private).

$$\mathcal{I}_{LIA}(Z_{val}^B) \triangleq \text{sign} \left(\sum_{z_{val} \in Z_{val}^B} L(z_{val}, \theta_t) - L(z_{val}, \theta_t^A) \right) \quad (1)$$

(iii) Finally, the center C aggregates the obfuscated votes $\mathcal{I}_{LIA}(Z_{val}^B)$ from all validators and filters out data with cumulative score *below a threshold* ($\sum_{\forall B} \mathcal{I}_{LIA}(Z_{val}^B) < T$). Specifically, we cluster the votes into two clusters (using k-means) and use the arithmetic mean of the cluster centers as the filtration threshold.

3.2.1 Advantages of the proposed lazy influence

Depending on the application, the designer may select any optimizer to perform the model updates. We do not require the loss function to be twice differentiable and convex; only once differentiable. It is significantly more *computation and communication efficient*; an essential prerequisite for any FL application. This is because participant A only needs to send (a *small part* of) the model parameters θ , not his training data. Moreover, computing a few model updates (using, e.g., SGD or any other optimizer) is significantly faster than computing either the exact influence or an approximation due to

Algorithm 1: Filtering Poor Data Using the Lazy Influence Approximation (LIA) in FL

```

1 for Data contributor  $A$  arriving at round  $t$  do
2    $A$ : Performs  $k$  local epochs with  $Z_{A,t}$  on the partially-frozen model  $\tilde{\theta}_t^A$ .
3    $A$ : Applies DP noise to  $\tilde{\theta}_t^A$ .
4    $A$ : sends last layer of  $\tilde{\theta}_t^A$  to a subset of the participants, that will be acting as validators.
5   for  $B_i$  in  $Validators(t)$  do
6      $B_i$ : Evaluates the loss of  $Z_{val}^{B_i}$  on  $\theta_t$  (current joint model of the federation)
7      $B_i$ : Evaluates the loss of  $Z_{val}^B$  on  $\tilde{\theta}_t^A$  (partially trained model from  $A$ )
8      $B_i$ : Calculates vote  $v$  (Lazy Influence Approximation), according to Equation 1
9      $B_i$ : Applies noise to  $v$  according to his privacy parameter  $p$  to get  $v'$  (Equation 2)
10     $B_i$ : Sends  $v'$  to  $C$  (private majority voting)
11   $C$ : Filters out ('rite of passage')  $A$ 's data if  $\sum_{\forall B_i} \mathcal{I}_{LIA}(Z_{val}^{B_i}) < T$ .
  
```

the numerous challenges. As a concrete example, computing the proposed LIA is *30 times faster* than the exact influence (on our simulations on real-data for Human Activity Recognition). Finally, and importantly, we ensure the *privacy* of both the train and validation dataset of every participant.

3.2.2 Sharing the Partially Updated Model: Privacy, Communication Cost, and Scalability

Each contributor A shares a partially trained model $\tilde{\theta}_t^A$ (see step (i) of Section 3.2). It is important to stress that A only sends the last layer of the model. This has two significant benefits. First, it minimizes the impact of the differential privacy noise. We follow [1, 66] to ensure strong datapoint-level local differential privacy guarantees by (i) imposing a bound on the gradient (using a clipping threshold Δ), and (ii) adding carefully crafted Gaussian noise (parameterized by σ). Second, it *reduces the communication overhead* (e.g., in our CIFAR simulations, *we only send 0.009% of the model's weights*). Moreover, as explained in the Introduction, this communication cost will be incurred only *once*, when we use our approach as a ‘right of passage’ every time a participant joins the federation. Importantly, in practice one can randomly select a (sufficiently large³) *subset* of validators, keeping the communication cost *constant* as we scale.

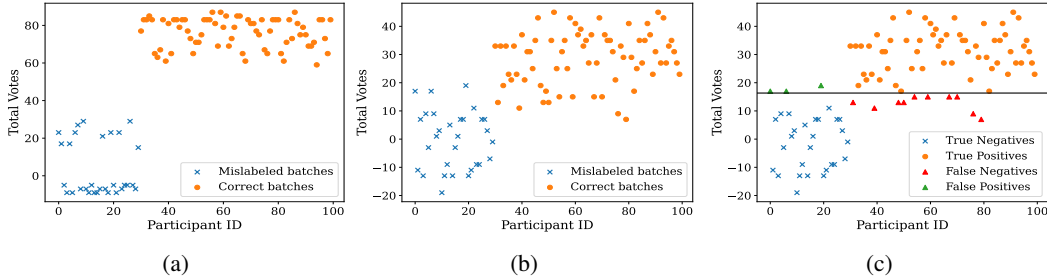


Figure 2: Visualization of the private voting scheme. The x -axis represents a contributor participant A . The y -axis shows the sum of all votes from all the validators, i.e., $\sum_{\forall B} \mathcal{I}_{LIA}(Z_{val}^B)$. Figure 2a corresponds to the sum of true votes (no privacy) for the validation data of each contributor on the x -axis, while Figure 2b depicts the sum of differentially private votes ($\epsilon = 1$), according to randomized reporting algorithm. Finally, Figure 2c shows the filtration threshold, corresponding to the arithmetic mean of the two cluster centers (computed using k -means).

3.2.3 Differentially Private Reporting of the Influence

Along with the training data, we also need to ensure the privacy of the validation data used to calculate the influence. Protecting the validation data in an FL setting is critical since (i) it is an important constraint of the FL setting, (ii) participants want to keep their sensitive information (and potential

³With enough votes, the aggregated LIA signs will match the sign of the true influence value in expectation. The size of the validators set is problem specific. See Sections 4, 4.3, and Figure 4.

means of income, e.g., in a crowdsourcing application) private, and (iii) the center wants to ensure that malicious participants can not tailor their contributions to the validation sets.

Each validator B_i is assigned a random ID number every time they act in that capacity. Moreover, each can split their test data into multiple *disjoint* sets, and then use each set *only once*.⁴ We obfuscate their influence reports using RAPPOR [22], which results in an ε -differential privacy guarantee [20].⁵ The obfuscation (permanent randomized response [59]) takes as input the participant’s true influence value v (binary) and privacy parameter p , and creates an obfuscated (noisy) reporting value v' , according to Eq. 2. p is a *user-tunable* parameter that allows the participants themselves to *choose their desired level of privacy*, while maintaining reliable filtering. The worst-case privacy guarantee can be computed by each participant *a priori*, using Eq. 3 [22].

$$v' = \begin{cases} +1, & \text{with probability } \frac{1}{2}p \\ -1, & \text{with probability } \frac{1}{2}p \\ v, & \text{with probability } 1 - p \end{cases} \quad (2) \quad \varepsilon = 2 \ln \left(\frac{1 - \frac{1}{2}p}{\frac{1}{2}p} \right) \quad (3)$$

It is important to note that in a Federated Learning application, the center C aggregates the influence sign from a *large number of participants*. This means that even under really strict privacy guarantees, *the aggregated influence signs (which is exactly what we use for filtering) will match the sign of the true value* in expectation. This results in high-quality filtering, as we will demonstrate in Section 4.

We visualize the obfuscation process in Figure 2, which shows the sum of true votes (y -axis) for the validation data of each contributor (x -axis). Here we can see a clear distinction in votes between corrupted and correct batches. Most of the corrupted batches (corrupted contributor participants) take negative values, meaning that the majority of the validators voted against them. In contrast, the correct batches are close to the upper bound. Figure 2b demonstrates the effect of applying DP noise ($\varepsilon = 1$) to the votes: differentiating between the two groups becomes more challenging. To find an effective decision threshold, we use k-means to cluster the votes into two clusters and use the arithmetic mean of the cluster centers as the filtration threshold (Figure 2c).

4 Evaluation Results

Dataset We evaluated the proposed approach on four well-established datasets: *CIFAR10* [36], *CIFAR100* [36], *real-data* on Human Activity Recognition (HAR) on edge devices [3, 2], and *real-data* on diagnosing heart conditions from X-rays [51]. Between these datasets, we evaluate on **two different modalities** (image data and sensor data), and **corruption of both the input \mathbf{X} , and the labels \mathbf{y}** . Due to lack of space, we focus on CIFAR in this section. Similar results were achieved for the other datasets. Please *see the Appendix for detailed results* (and also the bar plot in Figure 1).

Corruption Methods (i) **Random label**: a random label is sampled for every training point. Used for the IID setting (as it does not make sense to assign a random label to a highly skewed Non-IID setting). (ii) **Label shift**: Every correct label is mapped to a different label and this new mapping is applied to the whole training dataset. Used in both IID and non-IID settings.

Setup Our evaluation involves a single round of Federated Learning. A small portion of every dataset (around 1%) is selected as the ‘warm-up’ data used by the center C to train the initial model M_0 . Each participant has two datasets: a training batch (Z_A , see Section 3.2, step (i)), which the participant uses to update the model when acting as the contributor participant, and a validation dataset (Z_{val}^B , see Section 3.2, step (ii)), which the participant uses to estimate the sign of the influence when acting as a validator participant. As a concrete example, for the CIFAR simulations the ratio of these datasets is 2 : 1. The training batch size is 100 (i.e., the training dataset includes 100 points, and the validation dataset consists of 50 points). This means that, e.g., for a simulation with 100 participants, each training batch is evaluated on $50 \times (100 - 1)$ validation points, and that for each training batch (contributor participant A), the center collected $(100 - 1)$ estimates of the influence sign (Equation 1). See the Appendix for details on the HAR dataset. We report results when having 30% corrupt participants. Additional results (0%, 10%, 20%, 40%) can be found in the Appendix. For each corrupted batch, we corrupted 100% of the data points (similar results were achieved with

⁴E.g., in our applications, each of these sets required at most 50 points for the vote to be accurate.

⁵Note that RAPPOR provides significantly stronger privacy guarantees ($\delta = 0$) that what is normally deployed in modern systems. Thus, in practice, the privacy loss ε will be even lower if we allow $\delta > 0$.

90%). Each simulation was run *8 times*. We report average values and standard deviations. The proposed approach is **model-agnostic** and can be used with *any* gradient-descent-based ML method.

Non-IID Setting The main hurdle for FL is that not all data is IID. Heterogeneous data distributions are all but uncommon in the real world. To simulate non-IID data, we used the Dirichlet distribution to split the training dataset as in related literature [28, 40, 27, 68]. This distribution is parameterized by α , which controls the concentration of different classes (see the Appendix for a visualization). We report results for $\alpha \rightarrow 0.1$, as in related literature (e.g., [68]), see the Appendix for the rest. This translates to a *highly non-IID distribution*, e.g., with just 3 classes per participant for the HAR dataset.

Baselines We compare against four baselines. **(i) Corrupted model:** no sanitization (no filtering). **(ii) Oracle filtration:** ideal scenario where we know which participants contribute bad data. **(iii) KRUM** [5]: byzantine robustness technique that selects the best gradient out of the update based on a pair-wise distance metric. **(iv) Trimmed-mean** [65]: another byzantine robustness technique that takes the average of gradients instead of just selecting one, also based on a pair-wise distance metric. **(v) Centered-Clipping** [33]: state-of-the-art technique for byzantine robust aggregators. Importantly, we show that our filtration technique is not mutually exclusive with these aggregators, instead it is highly beneficial *in conjunction* to them (see Figure 3).

4.1 Model Performance

The proposed approach achieves *high model performance, close to the model performance of the perfect (oracle) filtering* (13.6% worse in the non-IID setting, and 0.1% in the IID setting). Focusing on the non-IID setting (Figure 3a), which is the more challenging and relevant for FL, our approach achieves a 10.8%, 20.3%, and 57.5% improvement over the Centered-Clipping, KRUM, and Trimmed-mean baselines, respectively, after 25 communication rounds. Interestingly, combining our approach with Centered-Clipping provides results almost as good as the Oracle filter (only 3% worse), which comes to show that LIA can *complement* Byzantine robustness techniques. Finally, while in the IID setting all methods perform similarly (Figure 3b), recall that the baselines do not provide privacy guarantees.

4.2 Filtration Metrics: Recall, Precision, Accuracy

Recall is the most informative metric to evaluate the efficiency of our filtering approach. Recall refers to the ratio of detected mislabeled batches over all of the mislabeled batches. *Including a mislabeled batch can harm a model’s performance significantly more compared to removing an unaltered batch.* Thus, achieving *high recall* is of paramount importance. Meanwhile, precision represents the ratio of correctly identified mislabeled batches over all batches identified as mislabeled. An additional benefit of using the proposed lazy influence metric for scoring data is that it also allows us to identify correctly labeled data, which nevertheless do not provide a significant contribution to the model. Finally, filtration accuracy refers to the ratio of correctly identified batches over all batches.

The proposed approach achieves both high recall and precision (Figure 4), despite the *high degree of non-IID* (low concentration of classes per participant). Notably, the metrics *improve significantly as we increase the number of participants* (horizontal axis, Figure 4). In simple terms, more validators mean more samples of the different distributions. Thus, ‘honest’ participants get over the filtering threshold, even in highly non-IID settings. Recall reaches 100% and precision 96.48% on CIFAR10 (Figure 4) by increasing the number of participants to just 500 (highly non-IID setting and under really strict worst-case privacy guarantees). Results for the IID setting are significantly better, with almost *perfect* recall, precision, and accuracy, even with only 100 participants.

4.3 Privacy

As expected, there is a trade-off between privacy and filtration quality (see Figure 4, vertical axis, where ϵ refers to the privacy guarantee for both the training and validation data/participant votes). Nevertheless, Figure 4 demonstrates that our approach can provide *reliable filtration*, even under *really strict, worst-case privacy requirements* ($\epsilon = 1$, which is the recommended value in the DP literature [54], $\delta = 10^{-5}$). Importantly, our decentralized framework allows each participant to *compute and tune his own* worst-case privacy guarantee *a priori* (see Section 3.2.3).

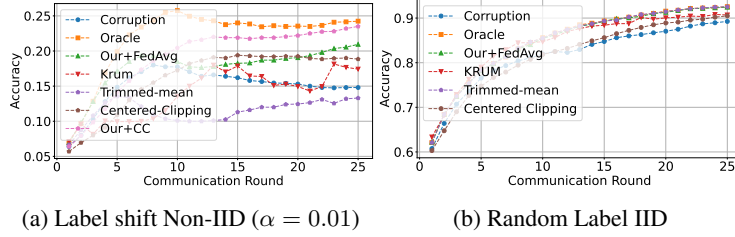


Figure 3: Model performance (model accuracy) over 25 communication rounds. 30% mislabel rate on CIFAR-10. The proposed (LIA) and oracle filters are used only *once* at the start (‘right of passage’ scenario). We compare a centralized model with no filtering (blue) to an FL model under perfect (oracle) filtering (orange), KRUM (red), Trimmed-mean (purple), Centered-Clipping (brown), our approach with FedAvg (green), and our approach with Centered-Clipping (pink). Note that the jagged line for KRUM is because only a single gradient is selected instead of performing FedAvg.

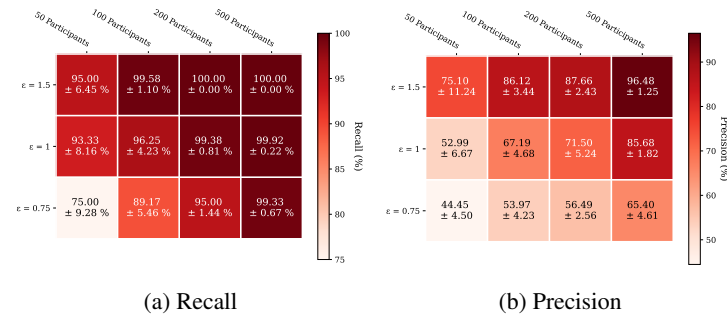


Figure 4: Recall and Precision on CIFAR 10, highly non-IID ($\alpha \rightarrow 0.1$), for increasing problem size (# of participants), and varying privacy guarantees (lower ϵ provides stronger privacy). $\delta = 10^{-5}$.

The *privacy trade-off can be mitigated*, and the quality of the filtration can be significantly improved by increasing the number of validators (Figure 4, horizontal axis). The higher the number of validators, the better the filtration (given a fixed number of corrupted participants). This is because as the number of validators increases, the aggregated influence signs (precisely what we use for filtering) will match the sign of the true influence value (in expectation). For 500 validators, we achieve high-quality filtration even for $\epsilon = 0.75$. This is important given that in most real-world FL applications, we *expect a large number of validators*.

4.4 Robustness

We evaluated our approach for varying mislabeling percentage (0%, 10%, 20%, 30%, 40%), varying levels of non-IID-ness ($\alpha = 0.1, 1, 10$), and a setting where not all data in a mislabeled batch are corrupt (90% corrupt). In all cases, the proposed approach enabled effective filtering (recall of $> 90\%$). Please see the Appendix for detailed results.

5 Conclusion

Privacy protection is a core element of Federated Learning. However, this privacy also means that it is significantly more difficult to ensure that the training data actually improves the model. Mislabeled, corrupted, or even malicious data can result in a strong degradation of the performance of the model (Figure 1) and privacy protection makes it significantly more challenging to identify the cause. We propose a *practical* influence approximation (‘*lazy influence*’) to be used as a ‘rite of passage’, allowing for effective filtering (recall of $> 90\%$, and even up to 100%), while providing *strict, worst-case* ϵ -differential privacy guarantees ($\epsilon \leq 1$) for both the training and validation data.

References

- [1] Martin Abadi, Andy Chu, Ian Goodfellow, H Brendan McMahan, Ilya Mironov, Kunal Talwar, and Li Zhang. Deep learning with differential privacy. In *CSS 2016 ACM SIGSAC*, 2016.
- [2] Davide Anguita, Alessandro Ghio, Luca Oneto, Xavier Parra, Jorge Luis Reyes-Ortiz, et al. Human activity recognition with smartphones dataset, 2013. <https://www.kaggle.com/datasets/uciml/human-activity-recognition-with-smartphones>.
- [3] Davide Anguita, Alessandro Ghio, Luca Oneto, Xavier Parra, Jorge Luis Reyes-Ortiz, et al. A public domain dataset for human activity recognition using smartphones. In *Esann*, volume 3, page 3, 2013.
- [4] Sean Augenstein, H Brendan McMahan, Daniel Ramage, Swaroop Ramaswamy, Peter Kairouz, Mingqing Chen, Rajiv Mathews, et al. Generative models for effective ml on private, decentralized datasets. *arXiv preprint arXiv:1911.06679*, 2019.
- [5] Peva Blanchard, El Mahdi El Mhamdi, Rachid Guerraoui, and Julien Stainer. Machine learning with adversaries: Byzantine tolerant gradient descent. In I. Guyon, U. Von Luxburg, S. Bengio, H. Wallach, R. Fergus, S. Vishwanathan, and R. Garnett, editors, *Advances in Neural Information Processing Systems*, 2017.
- [6] Sebastian Caldas, Sai Meher Karthik Duddu, Peter Wu, Tian Li, Jakub Konečný, H Brendan McMahan, Virginia Smith, and Ameet Talwalkar. Leaf: A benchmark for federated settings. *arXiv preprint arXiv:1812.01097*, 2018.
- [7] Xiaoyu Cao, Minghong Fang, Jia Liu, and Neil Zhenqiang Gong. Fltrust: Byzantine-robust federated learning via trust bootstrapping. *arXiv:2012.13995*, 2020.
- [8] Mingqing Chen, Rajiv Mathews, Tom Ouyang, and Françoise Beaufays. Federated learning of out-of-vocabulary words. *arXiv preprint arXiv:1903.10635*, 2019.
- [9] Christopher A Choquette-Choo, H Brendan McMahan, Keith Rush, and Abhradeep Thakurta. Multi-epoch matrix factorization mechanisms for private machine learning. *arXiv preprint arXiv:2211.06530*, 2022.
- [10] Andreas Christmann and Ingo Steinwart. On robustness properties of convex risk minimization methods for pattern recognition. *JMLR*, 2004.
- [11] R Dennis Cook and Sanford Weisberg. Characterizations of an empirical influence function for detecting influential cases in regression. *Technometrics*, 1980.
- [12] R Dennis Cook and Sanford Weisberg. *Residuals and influence in regression*. New York: Chapman and Hall, 1982.
- [13] Panayiotis Danassis, Aleksei Triastcyn, and Boi Faltings. A distributed differentially private algorithm for resource allocation in unboundedly large settings. In *Proceedings of the 21th International Conference on Autonomous Agents and MultiAgent Systems, AAMAS-22*. International Foundation for Autonomous Agents and Multiagent Systems, 2022.
- [14] Anirban Dasgupta, Petros Drineas, Boulos Harb, Ravi Kumar, and Michael W Mahoney. Sampling algorithms and coresets for ℓ_p regression. *SIAM Journal on Computing*, 2009.
- [15] Soham De, Leonard Berrada, Jamie Hayes, Samuel L Smith, and Borja Balle. Unlocking high-accuracy differentially private image classification through scale, 2022. *arXiv:2204.13650*, 2022.
- [16] Jia Deng, Wei Dong, Richard Socher, Li-Jia Li, Kai Li, and Li Fei-Fei. Imagenet: A large-scale hierarchical image database. In *2009 IEEE conference on computer vision and pattern recognition*, pages 248–255. Ieee, 2009.
- [17] Cynthia Dwork. Differential privacy. In *33rd International Colloquium on Automata, Languages and Programming, part II (ICALP 2006)*, volume 4052, pages 1–12, Venice, Italy, July 2006. Springer Verlag.

- [18] Cynthia Dwork. Differential privacy. In Michele Bugliesi, Bart Preneel, Vladimiro Sassone, and Ingo Wegener, editors, *Automata, Languages and Programming*, pages 1–12, Berlin, Heidelberg, 2006. Springer Berlin Heidelberg.
- [19] Cynthia Dwork, Krishnaram Kenthapadi, Frank McSherry, Ilya Mironov, and Moni Naor. Our data, ourselves: Privacy via distributed noise generation. In *Annual International Conference on the Theory and Applications of Cryptographic Techniques*, pages 486–503. Springer, 2006.
- [20] Cynthia Dwork, Frank McSherry, Kobbi Nissim, and Adam Smith. Calibrating noise to sensitivity in private data analysis. In *Theory of cryptography conference*, 2006.
- [21] Cynthia Dwork, Aaron Roth, et al. The algorithmic foundations of differential privacy. *Foundations and Trends in Theoretical Computer Science*, 9(3-4):211–407, 2014.
- [22] Úlfar Erlingsson, Vasyl Pihur, and Aleksandra Korolova. Rappor: Randomized aggregatable privacy-preserving ordinal response. In *Proceedings of the 2014 ACM SIGSAC conference on computer and communications security*, pages 1054–1067, 2014.
- [23] Amirata Ghorbani and James Zou. Data shapley: Equitable valuation of data for machine learning. In *International Conference on Machine Learning*, pages 2242–2251. PMLR, 2019.
- [24] Amirata Ghorbani and James Zou. Data shapley: Equitable valuation of data for machine learning. In Kamalika Chaudhuri and Ruslan Salakhutdinov, editors, *Proceedings of the 36th International Conference on Machine Learning*, volume 97 of *Proceedings of Machine Learning Research*, pages 2242–2251. PMLR, 09–15 Jun 2019.
- [25] Andrew Hard, Kanishka Rao, Rajiv Mathews, Swaroop Ramaswamy, Françoise Beaufays, Sean Augenstein, Hubert Eichner, Chloé Kiddon, and Daniel Ramage. Federated learning for mobile keyboard prediction. *arXiv preprint arXiv:1811.03604*, 2018.
- [26] Chaoyang He, Songze Li, Jinhyun So, Xiao Zeng, Mi Zhang, Hongyi Wang, Xiaoyang Wang, Praneeth Vepakomma, Abhishek Singh, Hang Qiu, et al. Fedml: A research library and benchmark for federated machine learning. *arXiv preprint arXiv:2007.13518*, 2020.
- [27] Haley Hoech, Roman Rischke, Karsten Müller, and Wojciech Samek. Fedauxfdp: Differentially private one-shot federated distillation, 2022.
- [28] Tzu-Ming Harry Hsu, Hang Qi, and Matthew Brown. Measuring the effects of non-identical data distribution for federated visual classification. *arXiv preprint arXiv:1909.06335*, 2019.
- [29] Ruoxi Jia, David Dao, Boxin Wang, Frances Ann Hubis, Nezihe Merve Gurel, Bo Li, Ce Zhang, Costas J Spanos, and Dawn Song. Efficient task-specific data valuation for nearest neighbor algorithms. *arXiv preprint arXiv:1908.08619*, 2019.
- [30] Ruoxi Jia, David Dao, Boxin Wang, Frances Ann Hubis, Nick Hynes, Nezihe Merve Gurel, Bo Li, Ce Zhang, Dawn Song, and Costas Spanos. Towards efficient data valuation based on the shapley value. In *AISTATS*, 2019.
- [31] Peter Kairouz, Brendan McMahan, Shuang Song, Om Thakkar, Abhradeep Thakurta, and Zheng Xu. Practical and private (deep) learning without sampling or shuffling. In *International Conference on Machine Learning*, pages 5213–5225. PMLR, 2021.
- [32] Peter Kairouz, H Brendan McMahan, Brendan Avent, Aurélien Bellet, Mehdi Bennis, Arjun Nitin Bhagoji, Kallista Bonawitz, Zachary Charles, Graham Cormode, Rachel Cummings, et al. Advances and open problems in federated learning. *Foundations and Trends® in Machine Learning*, 14(1–2):1–210, 2021.
- [33] Sai Praneeth Karimireddy, Lie He, and Martin Jaggi. Learning from History for Byzantine Robust Optimization. In *ICML 2021 - Proceedings of International Conference on Machine Learning*, 2021.
- [34] Shiva Prasad Kasiviswanathan, Homin K Lee, Kobbi Nissim, Sofya Raskhodnikova, and Adam Smith. What can we learn privately? *SIAM Journal on Computing*, 40(3):793–826, 2011.

- [35] Pang-Wei Koh and Percy Liang. Understanding black-box predictions via influence functions. In *International conference on machine learning*, pages 1885–1894. PMLR, 2017.
- [36] Alex Krizhevsky, Geoffrey Hinton, et al. Learning multiple layers of features from tiny images. *Learning Multiple Layers of Features from Tiny Images*, 2009.
- [37] Anran Li, Lan Zhang, Juntao Tan, Yaxuan Qin, Junhao Wang, and Xiang-Yang Li. Sample-level data selection for federated learning. In *IEEE INFOCOM 2021-IEEE Conference on Computer Communications*, pages 1–10. IEEE, 2021.
- [38] Tian Li, Anit Kumar Sahu, Ameet Talwalkar, and Virginia Smith. Federated learning: Challenges, methods, and future directions. *IEEE Signal Processing Magazine*, 37(3):50–60, 2020.
- [39] Wei Yang Bryan Lim, Nguyen Cong Luong, Dinh Thai Hoang, Yutao Jiao, Ying-Chang Liang, Qiang Yang, Dusit Niyato, and Chunyan Miao. Federated learning in mobile edge networks: A comprehensive survey. *IEEE Communications Surveys & Tutorials*, 22(3):2031–2063, 2020.
- [40] Tao Lin, Lingjing Kong, Sebastian U Stich, and Martin Jaggi. Ensemble distillation for robust model fusion in federated learning. *Advances in Neural Information Processing Systems*, 2020.
- [41] Ken Liu, Shengyuan Hu, Steven Z Wu, and Virginia Smith. On privacy and personalization in cross-silo federated learning. *Advances in neural information processing systems*, 35:5925–5940, 2022.
- [42] Xiaoxuan Liu, Livia Faes, Aditya U Kale, Siegfried K Wagner, Dun Jack Fu, Alice Bruynseels, Thushika Mahendiran, Gabriella Moraes, Mohith Shamdas, Christoph Kern, et al. A comparison of deep learning performance against health-care professionals in detecting diseases from medical imaging: a systematic review and meta-analysis. *The lancet digital health*, 1(6):e271–e297, 2019.
- [43] Yong Liu, Shali Jiang, and Shizhong Liao. Efficient approximation of cross-validation for kernel methods using bouligand influence function. In *ICML*, 2014.
- [44] Yuhan Liu, Ananda Theertha Suresh, Felix Xinnan X Yu, Sanjiv Kumar, and Michael Riley. Learning discrete distributions: user vs item-level privacy. *Advances in Neural Information Processing Systems*, 33:20965–20976, 2020.
- [45] Brendan McMahan, Eider Moore, Daniel Ramage, Seth Hampson, and Blaise Aguera y Arcas. Communication-efficient learning of deep networks from decentralized data. In *Artificial intelligence and statistics*, pages 1273–1282. PMLR, 2017.
- [46] H. Brendan McMahan, Daniel Ramage, Kunal Talwar, and Li Zhang. Learning differentially private recurrent language models. In *International Conference on Learning Representations*, 2018.
- [47] Sharada P Mohanty, David P Hughes, and Marcel Salathé. Using deep learning for image-based plant disease detection. *Frontiers in plant science*, 7:1419, 2016.
- [48] Luke Oakden-Rayner, Jared Dunnmon, Gustavo Carneiro, and Christopher Ré. Hidden stratification causes clinically meaningful failures in machine learning for medical imaging. In *Proceedings of the ACM conference on health, inference, and learning*, pages 151–159, 2020.
- [49] Luis Oala, Manil Maskey, Lilith Bat-Leah, Alicia Parrish, Nezihe Merve Gürel, Tzu-Sheng Kuo, Yang Liu, Rotem Dror, Danilo Brajovic, Xiaozhe Yao, et al. Dmlr: Data-centric machine learning research—past, present and future. *arXiv preprint arXiv:2311.13028*, 2023.
- [50] Kohei Ogawa, Yoshiki Suzuki, and Ichiro Takeuchi. Safe screening of non-support vectors in pathwise svm computation. In *ICML*, 2013.
- [51] Pranav Rajpurkar, Jeremy Irvin, Kaylie Zhu, Brandon Yang, Hershel Mehta, Tony Duan, Daisy Ding, Aarti Bagul, Curtis Langlotz, Katie Shpanskaya, et al. Chexnet: Radiologist-level pneumonia detection on chest x-rays with deep learning. *arXiv preprint arXiv:1711.05225*, 2017.

- [52] Jinhyun So, Başak Güler, and A Salman Avestimehr. Byzantine-resilient secure federated learning. *IEEE Journal on Selected Areas in Communications*, 2020.
- [53] Jun Tang, Aleksandra Korolova, Xiaolong Bai, Xueqiang Wang, and Xiaofeng Wang. Privacy loss in apple’s implementation of differential privacy on macos 10.12. *arXiv preprint arXiv:1709.02753*, 2017.
- [54] Aleksei Triastcyn. *Data-Aware Privacy-Preserving Machine Learning*. PhD thesis, EPFL, Lausanne, 2020.
- [55] Aleksei Triastcyn and Boi Faltings. Federated learning with bayesian differential privacy. In *IEEE International Conference on Big Data (Big Data)*. IEEE, 2019.
- [56] Tiffany Tuor, Shiqiang Wang, Bong Jun Ko, Changchang Liu, and Kin K Leung. Overcoming noisy and irrelevant data in federated learning. In *25th International Conference on Pattern Recognition (ICPR)*. IEEE, 2021.
- [57] Jianyu Wang, Zachary Charles, Zheng Xu, Gauri Joshi, H Brendan McMahan, Maruan Al-Shedivat, Galen Andrew, Salman Avestimehr, Katharine Daly, Deepesh Data, et al. A field guide to federated optimization. *arXiv preprint arXiv:2107.06917*, 2021.
- [58] Zhibo Wang, Mengkai Song, Zhifei Zhang, Yang Song, Qian Wang, and Hairong Qi. Beyond inferring class representatives: User-level privacy leakage from federated learning. In *IEEE INFOCOM 2019-IEEE conference on computer communications*, pages 2512–2520. IEEE, 2019.
- [59] Stanley L Warner. Randomized response: A survey technique for eliminating evasive answer bias. *Journal of the American Statistical Association*, 60(309):63–69, 1965.
- [60] Lauren Watson, Rayna Andreeva, Hao-Tsung Yang, and Rik Sarkar. Differentially private shapley values for data evaluation. *arXiv preprint arXiv:2206.00511*, 2022.
- [61] Bichen Wu, Chenfeng Xu, Xiaoliang Dai, Alvin Wan, Peizhao Zhang, Zhicheng Yan, Masayoshi Tomizuka, Joseph Gonzalez, Kurt Keutzer, and Peter Vajda. Visual transformers: Token-based image representation and processing for computer vision, 2020.
- [62] Yihao Xue, Chaoyue Niu, Zhenzhe Zheng, Shaojie Tang, Chengfei Lyu, Fan Wu, and Guihai Chen. Toward understanding the influence of individual clients in federated learning. In *Proceedings of the AAAI Conference on Artificial Intelligence*, volume 35, pages 10560–10567, 2021.
- [63] Tom Yan, Christian Kroer, and Alexander Peysakhovich. Evaluating and rewarding teamwork using cooperative game abstractions. *Advances in Neural Information Processing Systems*, 33:6925–6935, 2020.
- [64] Qiang Yang, Yang Liu, Tianjian Chen, and Yongxin Tong. Federated machine learning: Concept and applications. *ACM Transactions on Intelligent Systems and Technology (TIST)*, 10(2):1–19, 2019.
- [65] Dong Yin, Yudong Chen, Ramchandran Kannan, and Peter Bartlett. Byzantine-robust distributed learning: Towards optimal statistical rates. In Jennifer Dy and Andreas Krause, editors, *Proceedings of the 35th International Conference on Machine Learning*, Proceedings of Machine Learning Research. PMLR, 2018.
- [66] Ashkan Yousefpour, Igor Shilov, Alexandre Sablayrolles, Davide Testuggine, Karthik Prasad, Mani Malek, John Nguyen, Sayan Ghosh, Akash Bharadwaj, Jessica Zhao, Graham Cormode, and Ilya Mironov. Opacus: User-friendly differential privacy library in PyTorch. *arXiv preprint arXiv:2109.12298*, 2021.
- [67] Ashkan Yousefpour, Igor Shilov, Alexandre Sablayrolles, Davide Testuggine, Karthik Prasad, Mani Malek, John Nguyen, Sayan Ghosh, Akash Bharadwaj, Jessica Zhao, Graham Cormode, and Ilya Mironov. Opacus: User-friendly differential privacy library in pytorch. *CoRR*, abs/2109.12298, 2021.

- [68] Yaodong Yu, Alexander Wei, Sai Praneeth Karimireddy, Yi Ma, and Michael Jordan. TCT: Convexifying federated learning using bootstrapped neural tangent kernels. In Alice H. Oh, Alekh Agarwal, Danielle Belgrave, and Kyunghyun Cho, editors, *Advances in Neural Information Processing Systems*, 2022.

A Appendix / Supplemental Material

Contents

This appendix covers further details of our work, which have been omitted due to space limitations. Specifically:

1. In Section B we describe the methodology of our benchmarks.
2. In Section C we discuss the datasets used, the selected hyper-parameters, and other implementation details.
3. In Section D we describe the potential positive and negative societal impact of our work.
4. In Section E we briefly discuss the limitations of our work.
5. In Sections F we provide additional discussion of our simulation results.

B Setting

We consider a classification problem from some input space \mathcal{X} (e.g., features, images, etc.) to an output space \mathcal{Y} (e.g., labels). In a Federated Learning setting, there is a center C that wants to learn a model $M(\theta)$ parameterized by $\theta \in \Theta$, with a non-negative loss function $L(z, \theta)$ on a sample $z = (\bar{x}, y) \in \mathcal{X} \times \mathcal{Y}$. Let $R(Z, \theta) = \frac{1}{n} \sum_{i=1}^n L(z_i, \theta)$ denote the empirical risk, given a set of data $Z = \{z_i\}_{i=1}^n$. We assume that the empirical risk is differentiable in θ . The training data are supplied by a set of data holders.

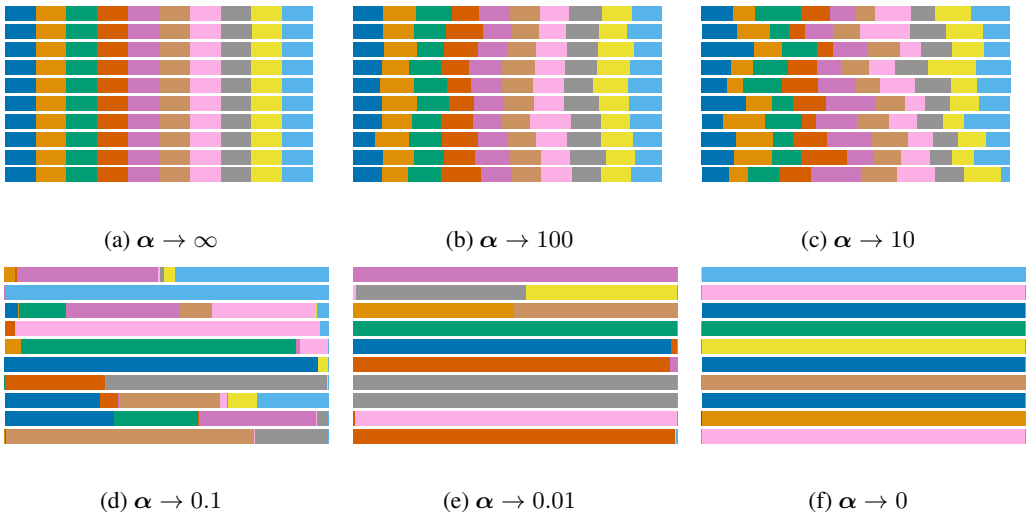


Figure 5: Dirichlet distribution visualisation for 10 classes, parametrized by α . α controls the concentration of different classes. Each row represents a participant, each color a different class, and each colored segment the amount of data the participant has from each class. For $\alpha \rightarrow \infty$, each participant has the same amount of data from each class (IID distribution). For $\alpha \rightarrow 0$, each participant only holds data from one class. In this work, we use $\alpha \rightarrow 0.1$ for a non-IID distribution.

B.1 Non-IID Setting

The main hurdle for Federated Learning is that not all data is IID. Heterogeneous data distributions are all but uncommon in the real world. To simulate a Non-IID distribution, we used Dirichlet distribution to split the training dataset as in related literature [28, 40, 27, 68]. This distribution is parameterized by α , which controls the concentration of different classes, as visualized in Figure 5. This work uses $\alpha \rightarrow 0.1$ for a non-IID distribution, as in related literature (e.g., [68]).

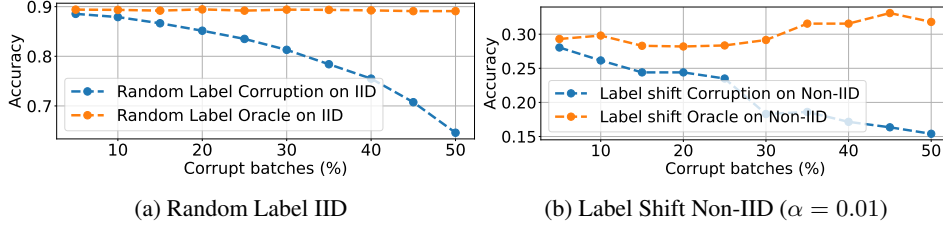


Figure 6: Model accuracy relative to different mislabel rates (5% - 50%). These models have been trained over 25 communication rounds and 100 participants. We compare a centralized model with no filtering of mislabeled data (blue) to an FL model under perfect (oracle) filtering (orange). Note that the lower accuracy on the Non-IID setting is due to the fact that we are considering the most extreme non-IID case. This is where the majority of the participants have access to at most 1 class.

B.2 Exact Influence

In simple terms, influence measures the marginal contribution of a data point on a model’s accuracy. A positive influence value indicates that a data point improves model accuracy, and vice-versa. More specifically, let $Z = \{z_i\}_{i=1}^n$, $Z_{+j} = Z \cup z_j$ where $z_j \notin Z$, and let

$$\hat{R} = \min_{\theta} R(Z, \theta) \quad \text{and} \quad \hat{R}_{+j} = \min_{\theta} R(Z_{+j}, \theta)$$

where \hat{R} and \hat{R}_{+j} denote the minimum empirical risk of their respective set of data. The *influence* of datapoint z_j on Z is defined as:

$$\mathcal{I}(z_j, Z) \triangleq \hat{R} - \hat{R}_{+j} \quad (4)$$

Despite being highly informative, influence functions have not achieved widespread use in Federated Learning (or Machine Learning in general). This is mainly due to the computational cost. Equation 4 requires complete retraining of the model, which is time-consuming, and very costly; especially for state-of-the-art, large ML models. Moreover, specifically in our setting, we do not have direct access to the training data. In the following section, we will introduce a practical approximation of the influence, applicable in Federated Learning scenarios.

B.3 Influence Approximation

The first-order Taylor approximation of influence, adopted by [35] (based on [12]), to understand the effects of training points on the predictions of a *centralized* ML model. To the best of our knowledge, this is the current state-of-the-art approach to utilizing the influence function in ML. Thus, it is worth taking the time to understand the challenges that arise if we adopt this approximation in the Federated Learning setting.

Let $\hat{\theta} = \arg \min_{\theta} R(Z, \theta)$ denote the empirical risk minimizer. The approximate influence of a training point z_j on the validation point z_{val} can be computed without having to re-train the model, according to the following equation:

$$\mathcal{I}_{appr}(z_j, z_{val}) \triangleq -\nabla_{\theta} L(z_{val}, \hat{\theta}) H_{\hat{\theta}}^{-1} \nabla_{\theta} L(z_j, \hat{\theta}) \quad (5)$$

where $H_{\hat{\theta}}^{-1}$ is the inverse Hessian computed on all the model’s training data. The advantage of Equation 5 is that we can answer counterfactuals on the effects of up/down-scaling a training point, without having to re-train the model. One can potentially average over the validation points of a participant, and/or across the training points in a batch of a contributor, to get the total influence.

B.4 Challenges

Consider Figure 6 as a motivating example. In this scenario, we have participants with corrupted data. Even a very robust model (ViT) loses performance when corruption is involved. This can also be observed in the work of [37]. Filtering those corrupted participants (orange line) restores the model’s performance.

	CIFAR10	CIFAR100	HAR
No. of Participants	100	100	500
Batch Size	100	250	2000
Validation Size	50	50	500
Random Factor	0.9	0.9	1.0
Warm-up Size	600	4000	7352
Final Evaluation Size	2000	2000	2947
Load Best Model	False	False	False
Parameters to Change	7690	76900	36358
Learning Rate	0.001	0.001	0.001
Train Epochs	3	3	20
Weight Decay	0.01	0.01	None

Table 1: Table of hyper-parameters.

While Equation 5 can be an effective tool in understanding centralized machine learning systems, it is *ill-matched* for Federated Learning models, for several key reasons.

To begin with, evaluating Equation 5 requires *forming and inverting* the Hessian of the empirical risk. With n training points and $\theta \in \mathbb{R}^m$, this requires $O(nm^2 + m^3)$ operations [35], which is *impractical* for modern-day deep neural networks with millions of parameters. To overcome these challenges, [35] used implicit Hessian-vector products (HVPs) to more efficiently approximate $\nabla_{\theta} L(z_{val}, \hat{\theta}) H_{\hat{\theta}}^{-1}$, which typically requires $O(p)$ [35]. While this is a somewhat more efficient computation, it is *communication-intensive*, as it requires *transferring all of the (either training or validation) data* at each FL round. Most importantly, it *can not provide any privacy* to the users’ data, an important, inherent requirement/constraint in FL.

Finally, to compute Equation 5, the loss function has to be strictly convex and twice differentiable (which is not always the case in modern ML applications). A proposed solution is to swap out non-differentiable components for smoothed approximations [35], but there is no quality guarantee of the influence calculated in this way.

C Implementation details

This section describes the base model used in our simulations and all hyper-parameters. Specifically, we used a Visual Image Transformer (VIT) [16, 61]. The basis of our model represents a model pre-trained on ImageNet-21k at 224x224 resolution and then fine-tuned on ImageNet 2012 at 224x224 resolution. All hyper-parameters added or changed from the default VIT hyper-parameters are listed in Table 1 with their default values. The following hyper-parameters have been added to support our evaluation technique:

- **Random Factor:** this coefficient represents the amount of corrupted data inside a corrupted batch.
- **Final Evaluation Size:** an a priori separated batch of test data to evaluate model performance.
- **Parameters to Change:** number of parameters (and biases) in the last layer of the model.

For the HAR dataset we have used a simple two-layer fully connected neural network. This network has not been pretrained like the previous one. With this network we chose to omit regularization and the detailed hyper-parameters are listed in Table 1. [67]

Regarding reproducibility, we ran the provided (in the supplementary material) code for each dataset with seeds from the range of 0 – 7.

C.1 Termination Condition

Different termination conditions have been used for our proposed solution and to retrain the exact influence. Our solution has only one termination condition, that is the number of local epochs k .

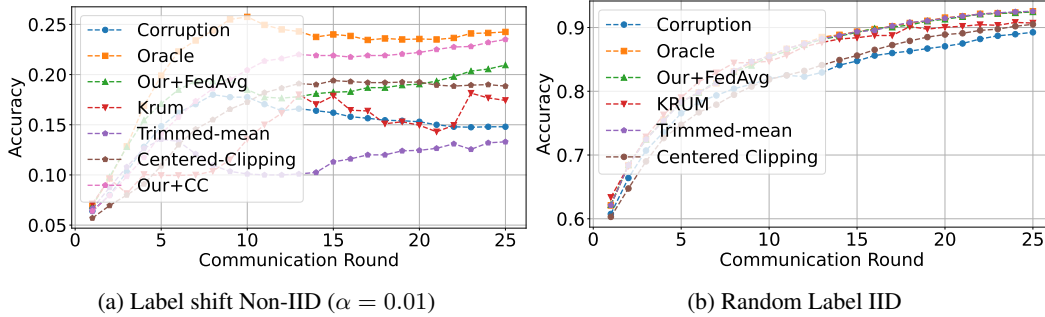


Figure 7: Model accuracy over 25 communication rounds with a 30% mislabel rate on CIFAR-10. We compare a centralized model with no filtering (blue) to an FL model under perfect filtering (orange), KRUM (red), Trimmed-mean (purple), and our approach (green). Note that the jagged line for KRUM is because only a single gradient is selected instead of performing FedAvg.

C.2 Computational Resources

All simulations were run on two different systems:

1. Intel Xeon E5-2680 – 12 cores, 24 threads, 2.5 GHz – with 256 GB of RAM, Titan X GPU (Pascal)
2. Ryzen 5900X - 12 cores, 24 threads, 3.7 GHz - with 32 GB of RAM, RTX 2080 Super

D Societal Impact

Privacy advocacy movements have, in recent years, raised their voices about the potential abuse of these systems. Additionally, legal institutions have also recognized the importance of privacy, and have passed regulations in accordance, for example, the General Data Protection Regulation (GDPR). Our work provides practical privacy guarantees to protect all parties, with minimal compromise on performance. Furthermore, we allow data holders and collectors to be paid for their contribution in a joint model, instead of simply taking the data. Such incentives could potentially help speed up the growth of underdeveloped countries, and provide more high-quality data to researchers (as an example application, consider paying low-income farmers for gathering data in crop disease prevention [47]).

E Limitations

The main limitation of our approach is that if the optimizer does not produce a good enough gradient, we cannot get a good approximation of the direction the model is headed for. The result of this is a lower score, and therefore a potentially inaccurate prediction.

Another potential limitation is the filtering of “good” data. These data may be correctly labeled, but including it does not essentially provide any benefit to the model, as can be shown by the accuracy scores in Figure 7. While this allows us to train models of equal performance with a fraction of the data, some participants may be filtered out, even though they contribute accurate data. This might deter users from participating in the future.

F Numerical Results

We provide detailed results that include both the means and standard deviations. The metrics can be found in Table 3. The following subsections provide a more comprehensive analysis of the results, summarized in the main text due to space limitations.

We have conducted initial testing on CIFAR10 and CIFAR100 to explore the impact of various parameters on our model’s performance. Our results, illustrated in Figures, 10, and 11 demonstrate the effect of both learning rate and number of epochs on filtration performance.

	Corruption				
	0%	10%	20%	30%	40%
Accuracy	85.2 +- 2.1 %	86.4 +- 1.2 %	87.2 +- 1.3 %	87.4 +- 1.1 %	89.0 +- 1.2 %
Recall	-	97.0 +- 0.5 %	96.4 +- 0.7 %	98.1 +- 0.6 %	97.5 +- 0.7 %

Table 2: Filtering performance on varying percentages of corrupt participants on the Human Activity Recognition dataset for *highly non-IID*. Following the same strict *worst-case differential privacy* guarantees ($\epsilon \leq 1, \delta = 10^{-5}$).

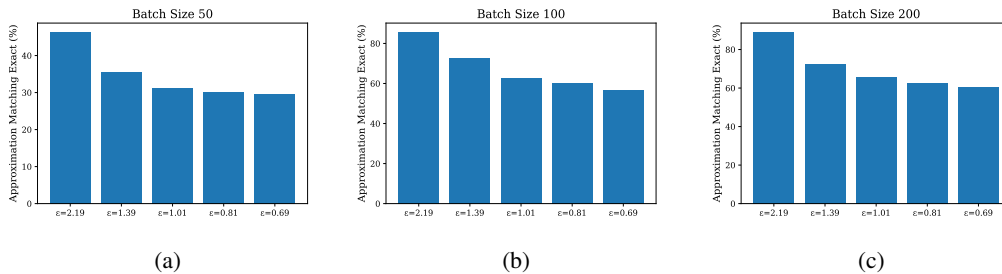


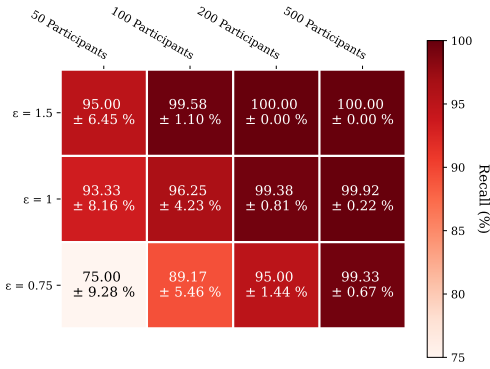
Figure 8: Effect of batch size to the percentage of the times the sign of the proposed Lazy Influence Approximation (LIA) matches the sign of the exact influence, for varying differential privacy guarantees (ϵ in the x -axis). Comparing 8a to the other two figures, we can observe that there is a certain threshold of data that needs to be passed for *lazy influence* to be effective. After this threshold has been reached, adding more data only gives marginal improvement as can be seen by comparing 8b and 8c.

		Filtration Metrics			
		Distribution	Recall	Precision	Accuracy
CIFAR 10	IID		97.08 \pm 3.51 %	91.91 \pm 7.15 %	96.38 \pm 2.83 %
	Non-IID		93.75 \pm 5.12 %	69.02 \pm 6.28 %	85.00 \pm 3.28 %
CIFAR 100	IID		99.17 \pm 2.20 %	97.96 \pm 2.30 %	99.12 \pm 1.27 %
	Non-IID		92.50 \pm 5.71 %	55.41 \pm 3.94 %	75.12 \pm 3.76 %
HAR	IID		100.00 \pm 0.0%	100.00 \pm 0.0%	100.00 \pm 0.0%
	Non-IID		95.77 \pm 2.1%	71.71 \pm 1.3%	87.40 \pm 1.1%

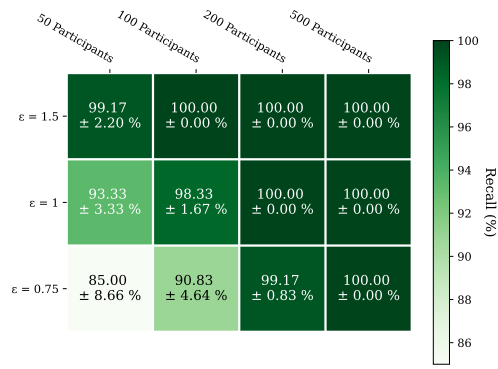
Table 3: Filtering performance on various datasets, including *real-data* on Human Activity Recognition, for IID and *highly non-IID* setting ($\alpha \rightarrow 0.1$, i.e., 3 classes per participant for HAR). 100 participants, 30% mislabeling rate. *Strict worst-case differential privacy* guarantees ($\epsilon \leq 1, \delta = 10^{-5}$).

We observe a balance between recall and accuracy that varies based on the parameters. This balance can be seen in both the CIFAR10 and CIFAR100 datasets. Additionally, the best parameters for IID and Non-IID may differ. For instance, the best recall for Non-IID and IID is achieved with different parameter pairs, and CIFAR100 also has a distinct parameter pair for IID compared to Non-IID.

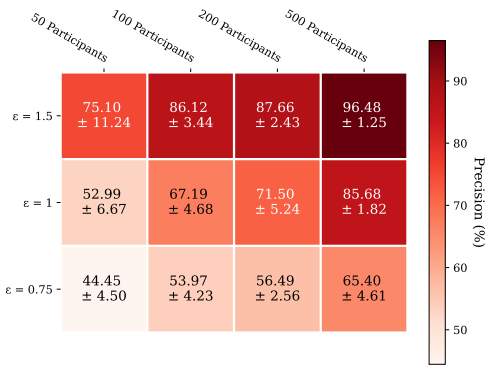
Finally, we examine the impact of various privacy guarantees (ϵ) and larger problem dimensions in Figure 9. Our findings show that a smaller federation is needed to achieve the same level of performance when data is IID, compared to when it is Non-IID.



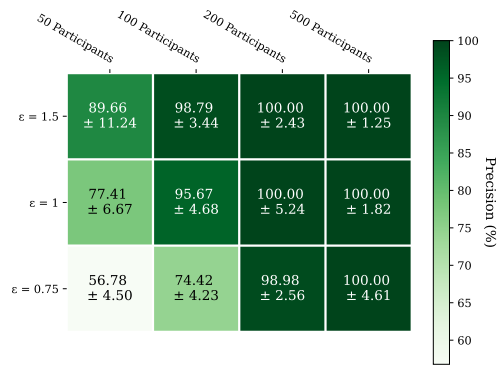
(a) Recall



(b) Recall



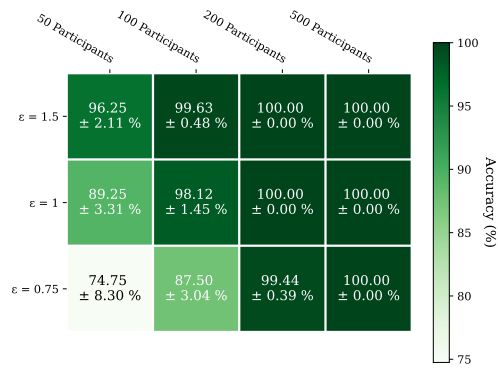
(c) Precision



(d) Precision

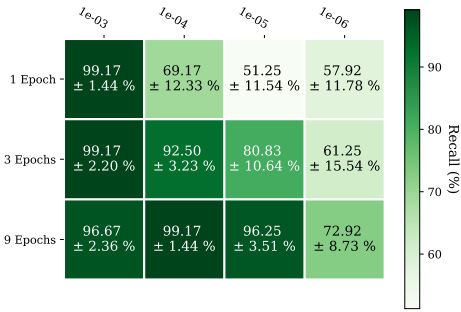


(e) Accuracy

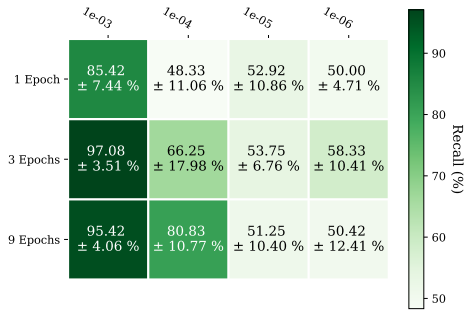


(f) Accuracy

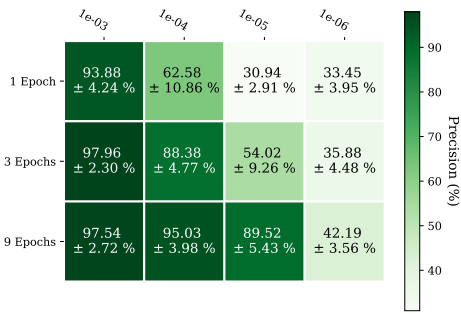
Figure 9: Recall (top), Precision (middle), and Accuracy (Bottom) on CIFAR 10, non-IID (left), IID (right), for increasing problem size (number of participants), and varying privacy guarantees (ϵ – lower ϵ provides stronger privacy).



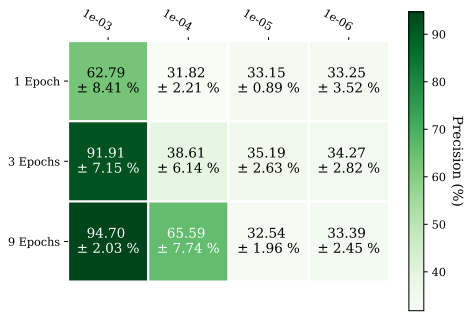
(a) Recall



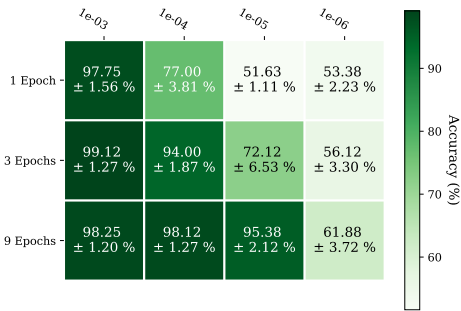
(b) Recall



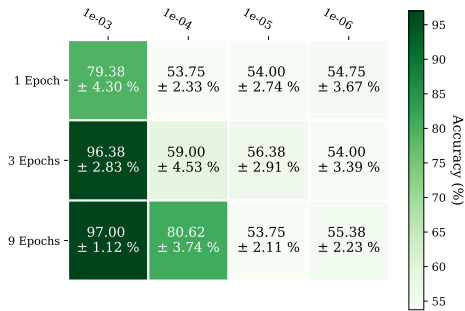
(c) Precision



(d) Precision

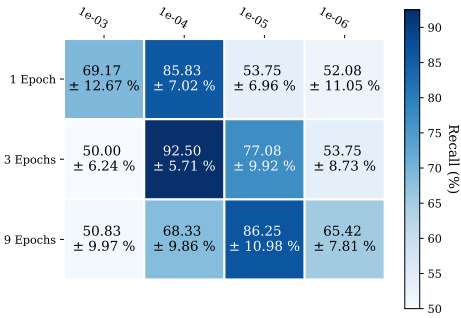


(e) Accuracy

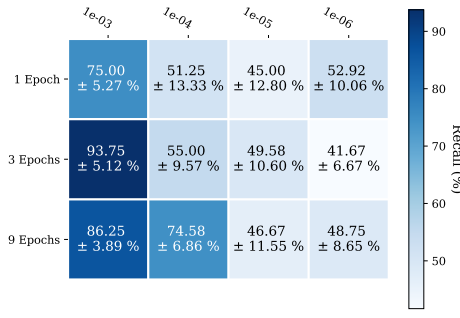


(f) Accuracy

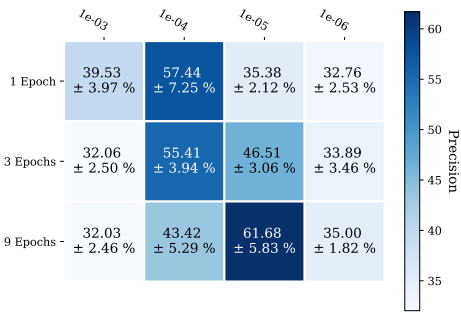
Figure 10: Recall (top), Precision (middle), and Accuracy (Bottom) on CIFAR 100 (left) and CIFAR 10 (right), IID, for different parameter pairs of learning rate and epoch count.



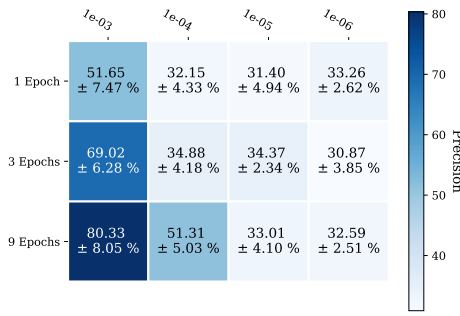
(a) Recall



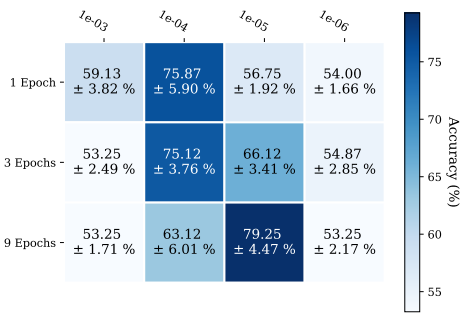
(b) Recall



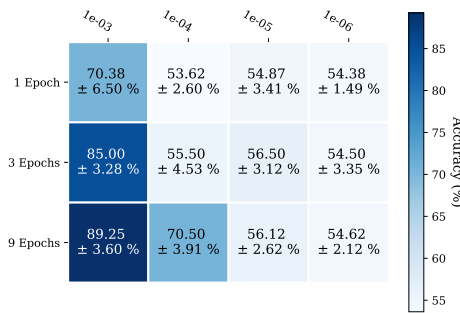
(c) Precision



(d) Precision



(e) Accuracy



(f) Accuracy

Figure 11: Recall (top), Precision (middle), and Accuracy (Bottom) on CIFAR 100 (left), and CIFAR 10 (right), non-IID, for different parameter pairs of learning rate and epoch count.